

Microdosimetry with a sealed mini-TEPC and a silicon telescope at a clinical proton SOBP of CATANA

Peer-reviewed author version

BIANCHI, Anna; Selva, A.; Colautti, P.; Bortot, D.; Mazzucconi, D.; Pola, A.; Agosteo, S.; Petringa, G.; Cirrone, G.A.P.; RENIERS, Brigitte; Paris, A.; Struelens, L.; Vanhavere, F. & Conte, V. (2020) Microdosimetry with a sealed mini-TEPC and a silicon telescope at a clinical proton SOBP of CATANA. In: RADIATION PHYSICS AND CHEMISTRY, 171 (Art N° 108730).

DOI: 10.1016/j.radphyschem.2020.108730

Handle: <http://hdl.handle.net/1942/30570>

Microdosimetry with a sealed mini-TEPC and a silicon telescope at a clinical proton SOBPs of CATANA

A. Bianchi^{a,b,c}, A. Selva^c, P. Colautti^c, D. Bortor^{d,e}, D. Mazzucconi^{d,e}, A. Pola^{d,e}, S. Agosteo^{d,e}, G. Petringa^f, G. A. P. Cirrone^f, B. Reniers^b, A. Parisi^a, L. Struelens^a, F. Vanhavere^a, V. Conte^c

^a Belgian Nuclear Research Centre, SCK•CEN, Boeretang 200, 2400 Mol, Belgium

^b UHasselt, Faculty of Engineering Technology, Centre for Environmental Sciences, Nuclear Technology Centre, Agoralaan, 3590 Diepenbeek, Belgium

^c Istituto Nazionale di Fisica Nucleare INFN, Laboratori Nazionali di Legnaro, viale dell'Università 2, Legnaro (Padova), Italy

^d Istituto Nazionale di Fisica Nucleare INFN, Sezione di Milano, via Celoria 16, Milano, Italy

^e Politecnico di Milano, Dipartimento di Energia, via La Masa 34, Milano, Italy

^f Istituto Nazionale di Fisica Nucleare INFN, Laboratori Nazionali del Sud, via Santa Sofia 62, Catania, Italy

Corresponding author: Anna Bianchi, anna.bianchi@sckcen.be

Abstract

A sealed miniaturized Tissue Equivalent Proportional Counter (mini-TEPC) able to work in gas-steady modality was developed at the Legnaro National Laboratories of the Italian National Institute of Nuclear Physics (LNL – INFN, Legnaro, Italy).

The aim of the present work is to compare the response of this mini-TEPC with that of a silicon microdosimeter based on a monolithic telescope.

Pairwise measurements were performed at the 62 MeV proton clinical Spread Out Bragg Peak (SOBP) of CATANA at the Southern National Laboratories of INFN (LNS – INFN, Catania, Italy). The dose mean lineal energy values were derived from the spectra measured with the two detectors and compared with the total dose-averaged *LET* calculated by means of Geant4 Monte Carlo simulations. Finally, the possibility to apply the Microdosimetric Kinetic Model (MKM) to reproduce RBE variations with depth along the spread out Bragg peak was investigated.

Keywords: Microdosimetry; Proton therapy; mini-TEPC; Silicon telescope; Beam quality

1. Introduction

Proton therapy is a cancer treatment modality that uses accelerated protons to treat tumours, instead of photons and electrons employed in conventional radiotherapy.

When protons are used, the physical dose has to be weighted for the corresponding Relative Biological Effectiveness (RBE) to take into account the different effect of proton radiation field on cells as compared to photons, for the same absorbed dose. In proton therapy a fixed RBE equal to 1.1 is mostly used, as recommended by the ICRU Report 78 [1]. However, an increasing RBE, reaching up to 1.7 in the fall-off of the SOBP, was found in several biological assays [2].

It has been demonstrated that the effectiveness of a radiotherapy treatment is mainly related to the local pattern of energy deposition at the subcellular level. More clustered energy deposition patterns result in lesions that are more difficult for the cell to repair [3]. A detailed physical knowledge of the local pattern of energy deposition is required for an accurate treatment planning, although the relation between the physical radiation interaction with the biological target and its effect is still difficult to establish [4, 5].

Microdosimetry is a valuable technique that measures the frequency distribution of stochastic quantities such as the lineal energy (y) imparted by the radiation field at the micrometre level [6]. The probability density $d(y)$ together with the dose averaged lineal energy, \bar{y}_D , are physical quantities correlated with the biological effectiveness of the therapeutic beam. Tissue Equivalent Proportional Counters (TEPC) are the reference devices in microdosimetry.

An alternative to TEPCs are the microdosimeters based on solid-state technologies like silicon detectors. Several measurements are reported in literature with silicon-on-insulator diode arrays of 10 μm of sensitive depth [7]. Being 10 μm thick, these silicon microdosimeters produce lineal energy spectra different from those measured at 1 μm or 2 μm , in particular in the distal part of a proton SOBP, where the low energy protons stop inside the detector sensitive volume.

Silicon-coated micro-thickness gauges have also been developed [8]. The size of their sensitive volume is only 2 μm giving the possibility of performing a beam characterization at a site size comparable to the one of the TEPCs. In general, silicon detectors are not tissue equivalent, therefore corrections are needed but at the same time their use is interesting for clinical applications because of their easy employment and fast use. A modified mini-TEPC able to work in gas-steady modality was developed at the LNL – INFN [9] and measurements with this detector were performed at CATANA beam line at LNS – INFN. In the same measurement campaign, a silicon detector has measured at the same depths of the mini-TEPC. A comparison between the beam characterization performed with the two detectors in terms of shape of the spectra and \bar{y}_D values compared with the total dose-averaged LET calculated with Monte Carlo simulations is presented in this paper. A similar comparison in terms of shape of the spectra was performed in [10], in that case, a different mini-TEPC was employed and the SOBP was different.

The main aim of this paper, after having evaluated that the shape of the spectra measured by both detectors is comparable, is to check how the two microdosimeters behave as radiation quality monitors. Therefore, \bar{y}_D values have been compared with the total dose-averaged LET in order to check the feasibility of using these microdosimeters as LET monitors.

Moreover, an RBE assessment was performed for both detectors applying the modified Microdosimetric Kinetic Model [11]. The RBE calculated with the MKM has been confronted with the RBE obtained for the U87 cell line in the same radiation field [12].

2. Materials and Methods

2.1 The sealed mini-TEPC

The new mini-TEPC is based on the design of the detector described in [13]. The geometry and constructive materials are the same but the gas ducts have been enlarged in order to facilitate the vacuum and gas cleaning procedures. The sensitive volume is a cylinder with equal diameter and height of 0.9 mm, the anode is a 10 μm gold-plated tungsten wire; the cathode wall is made of 0.35 mm thick conductive A150 tissue-equivalent plastic, and it is surrounded by an insulating 0.35 mm layer of Rexolite®. The sensor stands inside a 0.2 mm thick and 150 mm long titanium sleeve. The total external diameter is 2.7 mm. The PMMA-equivalent wall thickness of the detector is 1.18 mm, as it results by taking into account the average stopping-power ratio of protons in the energy range from 5 MeV to 62 MeV within the different materials. A drawing of the mini-TEPC is shown in Figure 1.

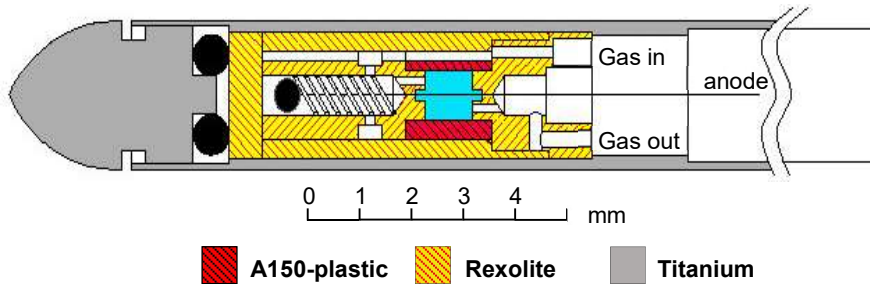


Fig. 1 – Transversal scheme of the new mini-TEPC, in light blue the sensitive volume.

After an optimized cleaning and filling procedure the detector was sealed at an internal pressure of 45.4 kPa of pure propane. It corresponds to a site size of 0.75 μm in pure propane with density 1 g/cm^3 which is equivalent to 1 μm in tissue – equivalent propane as explained in [14] or to 0.85 μm in water dividing by factor equal to 0.88 ± 0.03 for the conversion from propane to water, as it results from the average mass stopping power ratio of protons in water and propane [15].

2.2 The silicon telescope

The silicon device consists of a ΔE stage composed by a matrix of micrometric cylindrical diodes of 2 μm of thickness and 9 μm of diameter, the pitch between the diodes is 41 μm . Each element of the matrix is surrounded by a guard-ring of 14 μm of diameter that confines the charge collection within the lateral surface of the sensitive volume. The E stage is 500 μm thick. E and ΔE stages are fabricated on a single silicon substrate and separated by a deeply implanted p+ cathode [10]. Each diode of the ΔE stage is a solid state microdosimeter while the E stage records the initial energy of the incident protons, when their residual range is less than the sensor thickness (i.e., for protons up to 8 MeV of energy).

2.3 Data Processing

The mini-TEPC measurements were performed biasing the cathode at -700 V and keeping the anode grounded through the pre-amplifier. The high gas gain and the low noise conditions were good enough to acquire lineal energy events down to 0.4 keV/ μm .

Three spectroscopy amplifiers were used to collect the signal in order to increase the spectra resolution; the obtained sub-spectra were then joint offline in a single spectrum. The joint spectrum is calibrated in lineal energy by fitting the proton edge with a Fermi-like function [16], the proton edge is clearly visible in the spectrum at 30.84 mm and it is related to the maximum energy that protons can release inside the sensitive volume. The maximum energy deposit in our sensitive volume according to Ion Stopping and Range Tables of SRIM [15] is approximately 96 keV in gaseous propane corresponding to a lineal energy value of 162 keV/ μm when divided by the mean chord length equal to $\frac{\pi}{4}d$ for a cylinder of diameter d irradiated transversally by a mono-directional beam. This value is then multiplied by the mean mass stopping power ratio of water to propane, $S_m^{(\text{water})}/S_m^{(\text{propane})}$, which is evaluated as 0.88 according to SRIM [15], in order to relate the calibration to liquid water. The resulting value of 143 keV/ μm for the proton-edge is then assigned to the inflection point of the Fermi-like function.

As far as the silicon telescope is concerned, both the E and ΔE stages were biased and the signals were collected separately in two different electronic chains. The amplified and shaped signals are acquired by a two-channel ADC in coincidence mode in order to keep the time correlation between the E and ΔE stage signals. The microdosimetric spectra obtained from the silicon telescope in the ΔE stage were analysed using the same procedure explained in [10]. The calibration of the output signal in terms of energy imparted was performed using the usual procedure for silicon devices: the capacitance of the silicon telescope was used to convert the signal voltage into a charge signal and then the energy gap of silicon semiconductors was used to calculate the energy deposit. The energy spectra were then corrected for water-equivalence to obtain lineal energy distributions in a water equivalent thickness and for the geometrical effect to take into account the different chord length distributions in the sensitive volumes[10]. In the proximal and plateau regions, up to the Bragg peak (approximate proton energy 10 MeV), the water equivalence correction was performed by scaling the energy deposited in the silicon by a constant factor: $\zeta=0.574$. In the distal region an event-by-event correction was applied, multiplying the energy deposited in silicon by the ratio of the stopping powers:

$$\varepsilon_i^{\text{water}} = \varepsilon_i^{\text{Si}} \cdot \frac{S^{\text{water}}(E_i)}{S^{\text{Si}}(E_i)} \quad (1)$$

Where ε_i is the energy of the impinging proton for the i -th event.

The frequency spectra $f(y)$ were linearly fitted between 0.4 and 0.5 keV/ μm for the mini-TEPC and between 8 and 8.5 keV/ μm for the silicon telescope, just above the noise threshold levels. The $f(y)$ spectra were then

linearly extrapolated down to 0.01 keV/ μm and processed to obtain the $yd(y)$ against the $\log(y)$ distribution and the \bar{y}_D value. More details on the extrapolation procedure can be found in literature [17].

2.4 Dose-averaged LET simulations

HADRONTHERAPY [18], which is a free and open source application available in the public release of the Geant4 [19] Monte Carlo code, is used to simulate the CATANA beamline. A new module has been implemented with respect to the one described in [20] in the HADRONTHERAPY application. Thanks to this new implementation *LET* distribution can be simulated in interesting configuration for radiobiological experiments. New algorithms were developed to produce results that are independent from the simulation transport parameters, i.e. voxel size, secondary particle threshold or step length [21]. In this work the new module was used to calculate the total dose-averaged *LET* (\overline{LET}_d) of the modulated Bragg Peak used in these measurements. The \overline{LET}_d values at each water depth the dose-averaged *LET* values for each particle have been weighted with their dose contribution, the following equation was used:

$$LET_d(z) = \frac{\sum_{j=1}^n \int_0^{\infty} S_{el}^{j^2}(E) \varphi_E^j(z) dE}{\sum_{j=1}^n \int_0^{\infty} S_{el}^j(E) \varphi_E^j(z) dE} \quad (2)$$

Where $LET_d(z)$ is the LET_d at the depth z in water, S_{el}^j is the electronic stopping power of a particle j with energy E and $\varphi_E^j(z)$ is the number of particles of type j that have energy E at depth z . The integral is done over the whole range of energies of the particle j and then the sum is performed over all charged particles set in motion by the primary protons. This new tool allows to calculate the dose-averaged *LET* considering both primary and secondary particles created by non-elastic nuclear interactions. In this case the dose-averaged *LET* is indicated with total- LET_d otherwise with primary- LET_d .

2.5 Measurement set-up

The CATANA beam line at the LNS – INFN is a 62 MeV proton beam that uses a passive half-modulated SOBP to treat ocular melanomas [22].

Measurements were performed at 11 positions along a 1.1 cm SOBP (see fig. 1) by sequentially adding different PMMA layers of 0.3 mm of thickness in front of the detectors. The conversion from depth in PMMA to depth in water was performed applying a factor of 1.16 ± 0.03 , determined as the average stopping power ratio of protons with energy between 5 MeV and 62 MeV. The values of the proton stopping power were assessed using SRIM [15].

Detectors were centred at the beam isocentre. The effective depth of the positions of the mini-TEPC was calculated adding 1.18 mm to the physical thickness of the PMMA stack. This value corresponds to the equivalent thickness of the mini-TEPC walls converted to PMMA using the average mass stopping power ratio for the different materials. A 1.18 mm thick layer of PMMA was also added to the stack when

measuring with silicon device to take into account for the mini-TEPC equivalent thickness. The uncertainty on the depth position was evaluated for both detectors as 0.15 mm.

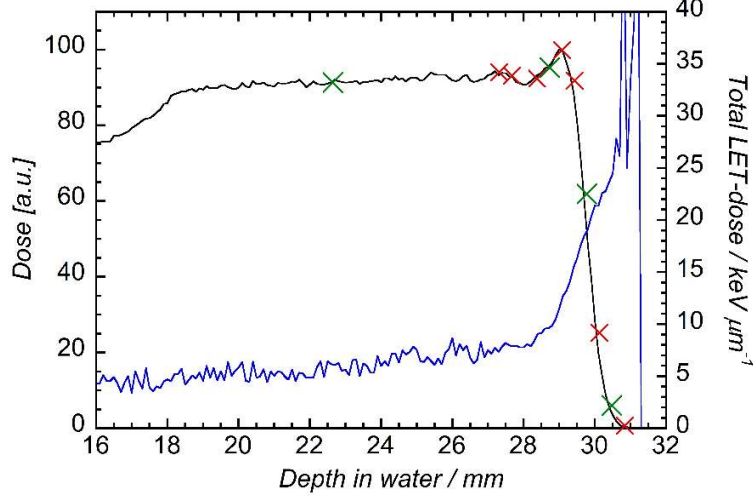


Fig. 2. – Clinical SOBP of CATANA. Dose profile measured with the Markus chamber in black, total LET-dose from MC simulation in blue. Crosses indicate positions at which both detectors measured (positions of the spectra shown in fig. 3 are marked with green crosses).

2.6 RBE assessment with the modified MKM

The modified Microdosimetric Kinetic Model correlates the probability of survival of a cell after irradiation (S) to the number of lethal lesions induced by ionizing radiations (L) and to the dose averaged lineal energy calculated by taking into account a saturation effect (y^*), and it integrates these parameters in the LQ model:

$$S = \exp(-L) = \exp(-\alpha D - \beta D^2) = \exp\left[-\left(\alpha_0 + \frac{\beta}{\rho\pi r_d^2} y^*\right) D - \beta D^2\right] \quad (3)$$

Where α_0 is the intercept of the linear fit of the plot of α_p as a function of y^* which is calculated as follows:

$$y^* = \frac{y_0 \int [1 - \exp(-y^2/y_0^2)] f(y) dy}{\int y f(y) dy} \quad (4)$$

$y_0 = 124 \text{ keV}/\mu\text{m}$ is used as saturation value for protons, as first indicated by Kellerer in [23] and then recommended in the ICRU report 36 [6].

3. Results and discussion

Spectra were compared in shape in four common positions along the SOBP. In figure 3 the normalized spectra of the mini-TEPC are shown together with the spectra of the silicon telescope before the linear extrapolation to low y values. The spectra of the silicon detector are not normalized but only scaled in order to show the superimposing parts with the mini-TEPC spectra.

It is possible to observe that the lower threshold for the silicon detector is around $8.5 \text{ keV}/\mu\text{m}$. This high threshold prevents the silicon telescope from measuring in the entrance part of the SOBP; significant spectral

information is recorded only in the distal part of the SOBP, as it can be seen in figure 3. However, the agreement of the common parts is good.

A small peak can be seen in the p-edge in the spectra at 30.13 mm and 30.84 mm acquired by the silicon microdosimeter. Such a peak was also observed in the spectra measured by another silicon detector, the MicroPlus 3D Bridge microdosimeter, which is an array of silicon sensitive volumes with an area of $30 \times 30 \mu\text{m}^2$ and a thickness of $10 \mu\text{m}$ [24]. Moreover, it was also found in [25] for different materials and it seems to be related to the geometry of the sensitive volume: it is present when the spectra are gathered with a planar detector orthogonal to the direction of the beam. However, its origin is still under investigation.

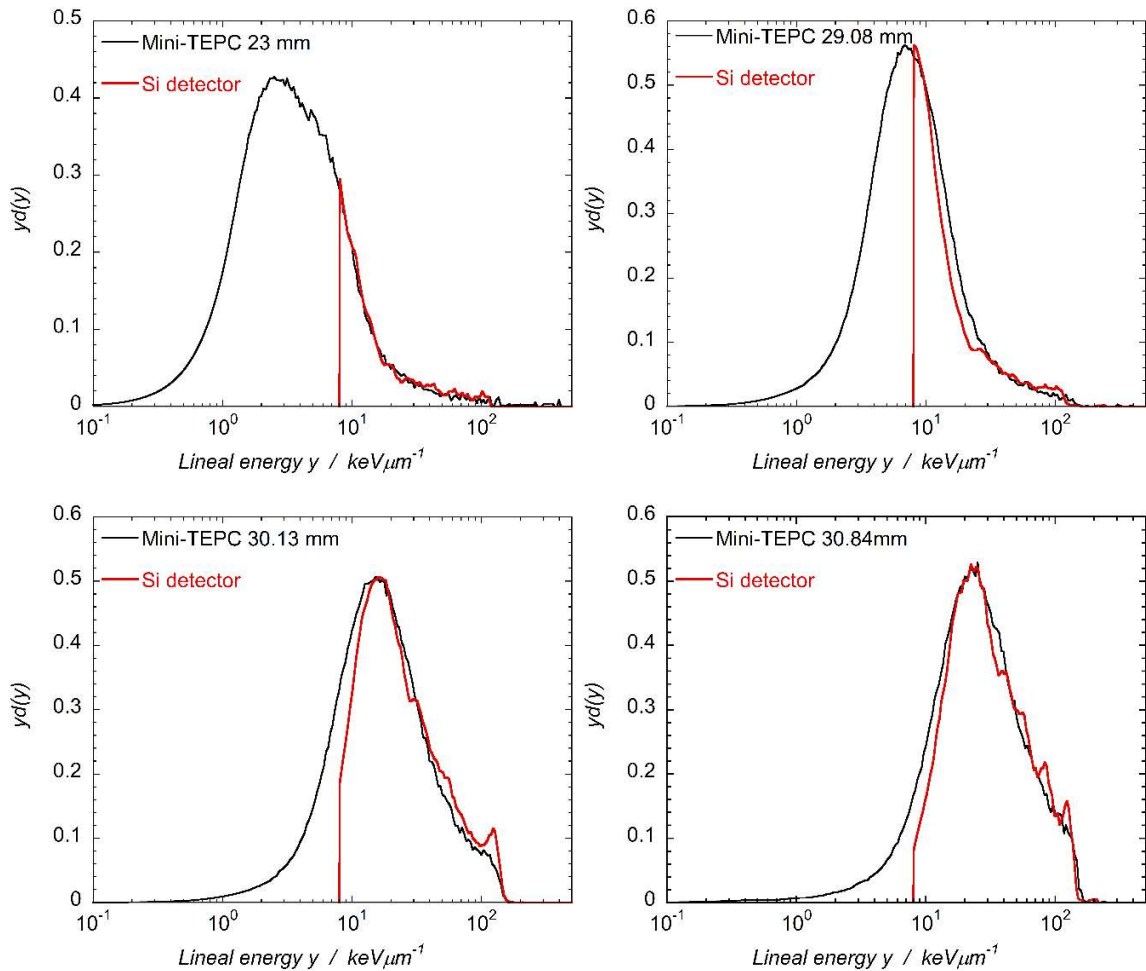


Fig. 3. Normalized spectra of the mini-TEPC (black) and spectra before linear extrapolation of the silicon telescope (red).

Similar results were already observed in [10]; what was confirmed by this measurement campaign is that the silicon detector can reproduce the spectra gathered with the new sealed mini-TEPC in the distal part of the SOBP but, due to the high threshold, it is not possible to measure the entire spectral information in the plateau and in the entrance part of it. A possible solution to this problem may be to use a thicker silicon telescope in the entrance part of the SOBP like those employed in [24]. In this region the total *LET*-dose

variations along a thickness of 10 μm are small because protons have high energy and they do not stop inside the sensitive volume, so a thicker detector does not affect the microdosimetric characterization of the beam. At the same time, it would allow to lower the detection threshold since the signal released by the particle inside the detector is bigger. A new kind of silicon telescope consisting of a stack of several layers of silicon detectors of different thickness might be developed in order to optimize the accuracy of measurements along the whole SOBP. Another possibility to reduce the noise level is to increase the number of pixels in order to increase the signal to noise ratio.

Moreover, studies are ongoing to investigate the use of silicon detectors based on avalanche diodes in microdosimetry. The presence of an internal gain might be a solution to increase the signal to noise ratio without increasing the thickness of the sensitive volume.

The silicon microdosimeter $yd(y)$ spectra, extrapolated down to 0.01 $\text{keV}/\mu\text{m}$, are shown in figure 4 and compared to the mini-TEPC spectra.

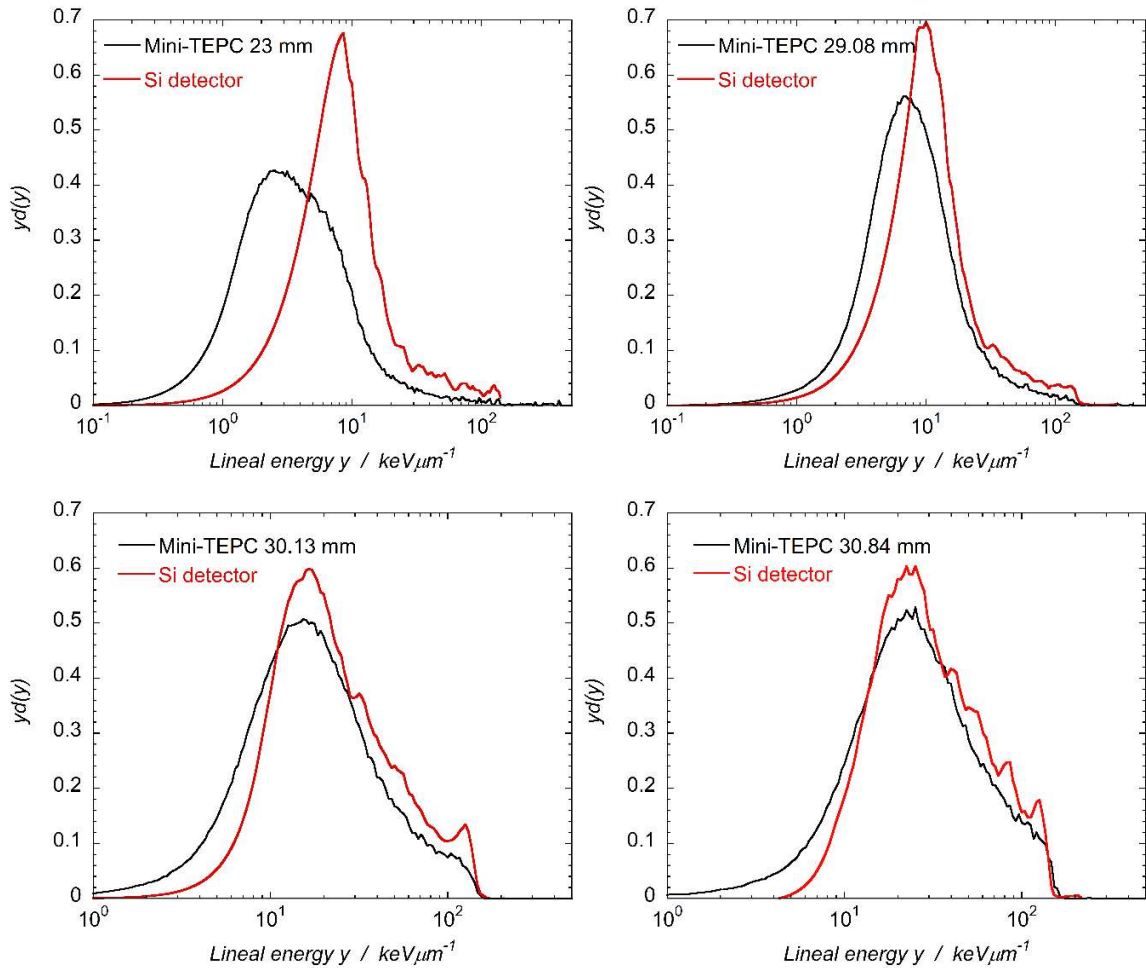


Fig. 4. Normalized spectra obtained with the mini-TEPC (black) and the silicon telescope (red).

It was found that the lineal energy distribution measured by the mini-TEPC is always larger than that of the silicon detector especially at low lineal energy values. This effect can be related both to the chord length distribution of the mini-TEPC (the silicon detector can be considered as a slab orthogonal to the beam direction), and to the wall effect of the TEPC: due to the presence of a wall with much higher density, the contribution of δ rays is bigger since those generated near the wall surface can enter the sensitive volume. In figure 5 a selection of 9 spectra acquired in the distal part of the SOBP for both detectors is shown.

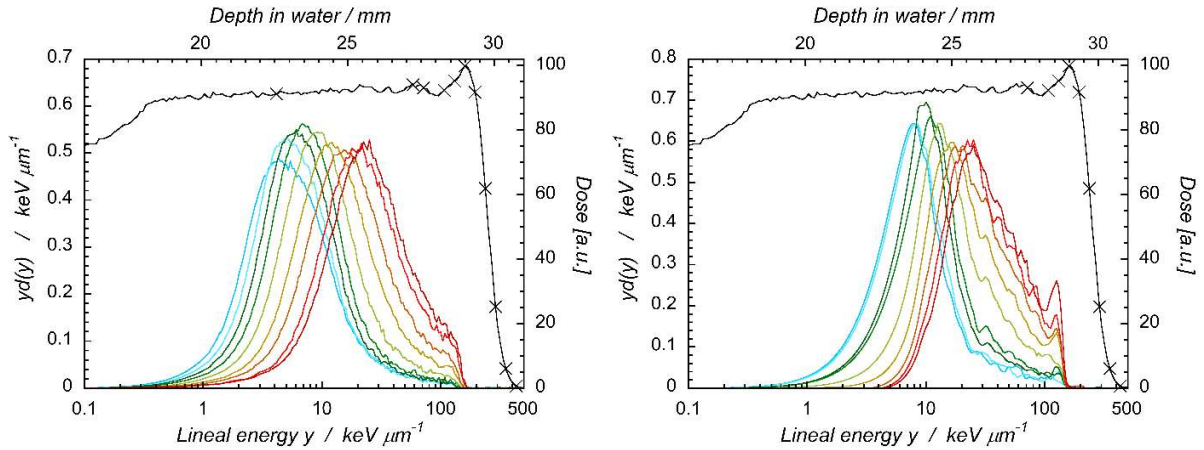


Fig. 5. Selection of 9 spectra acquired in the distal part of the SOBP with the mini-TEPC (left) and the silicon telescope (right).

From the analysis of the spectra in figure 5, both detectors are able to measure the variations between two consecutive spectra that are acquired at 0.3 mm of depth one from the other in PMMA, equal to 0.35 mm in water. Defining the spatial resolution as the capability of appreciate the difference between two measured spectra, it is possible to assess that both detectors have a spatial resolution smaller than 0.35 mm in water, especially in the distal part of the SOBP where the radiation quality changes faster.

Starting from the extrapolated spectra the dose mean lineal energy was calculated in order to compare the microdosimetric results with the total dose-averaged LET calculated with the Monte Carlo code Geant4, the results are shown in figure 6.

The \bar{y}_D values obtained with the silicon telescope overestimate the total LET -dose, even if the general trend of the data is comparable. A unique scaling factor of 0.65 was therefore applied to the data, obtained as the average of the ratios of the total LET -dose and the measured \bar{y}_D at the points of measurement. This factor was used to shift all the dose mean lineal energy values measured by the silicon microdosimeter, obtaining a good agreement.

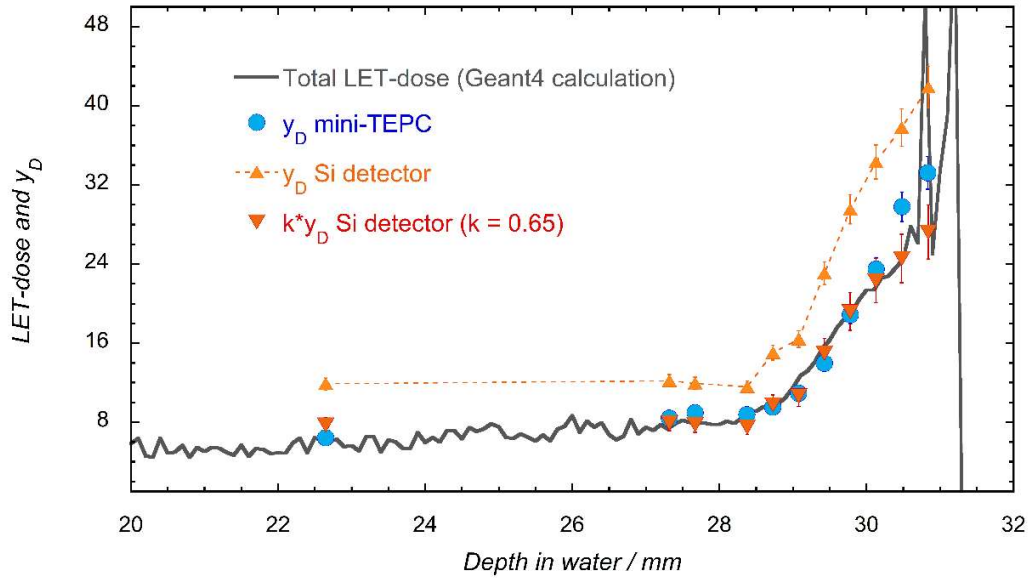


Fig. 6. \bar{y}_D values measured by the mini-TEPC (O), and by the silicon detector before applying the scaling factor (Δ) and after (∇). The grey solid line is the total LET_D calculated with Geant4.

RBE at 10% of survival was calculated using the modified Microdosimetric Kinetic Model. Radiobiological measurements [12] were performed in the same beam but using a different modulator. In order to be able to compare them with microdosimetric results, the dose profile was calibrated at the R80 resulting in a shift of 0.9 mm backwards on the cells positions (see fig.7).

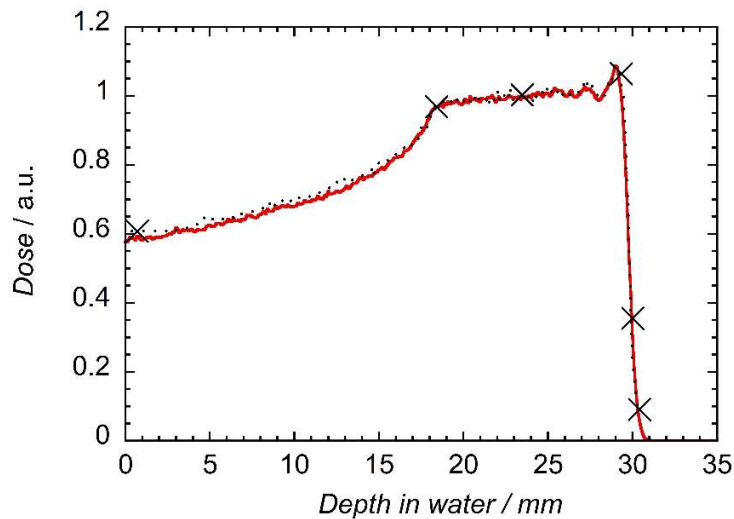


Fig. 7 – Dose profiles calibrated at the same R80. In red the SOBP profile of this experiments, the black dotted line is the shifted profile of the biological measurements in [12], crosses represents the positions of biological assays.

Figure 8 shows the α_p obtained by the linear fitting of the survival curves published in [12] and the y^* data resulting from the microdosimetric measurements with both detectors in the same positions in which biological data were gathered. The parameters coming from the linear fit were then used as input data for

the MKM. The input parameters found for the mini-TEPC are: $r_d = 0.29 \mu\text{m}$, $\alpha_0 = 0.028356 \text{ Gy}^{-1}$ and for the silicon telescope: $r_d = 0.31 \mu\text{m}$, $\alpha_0 = -0.13494 \text{ Gy}^{-1}$. For the U87 cell line $\alpha_x = 0.11 \text{ Gy}^{-1}$ and it was assumed that $\beta_p = \beta_x = 0.06 \text{ Gy}^{-2}$ as usually done in the MKM [12]. No scaling factors were used on the y^* obtained from the silicon telescope.

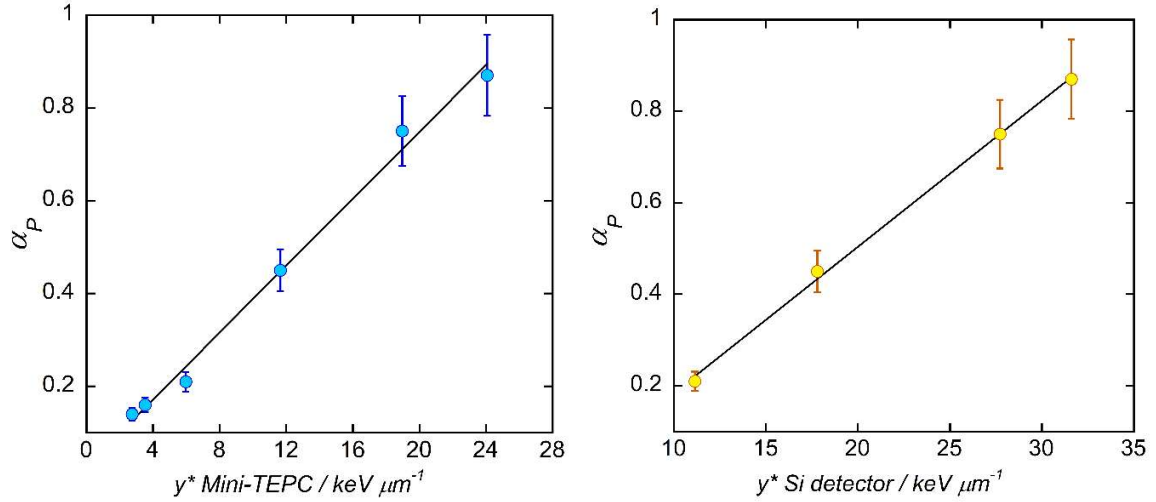


Fig. 8. – Linear fit of α_P as a function of y^*

In figure 9 the RBE10 obtained for the mini-TEPC and the silicon detector with the MKM are shown together with the RBE10 of the U87 cell line.

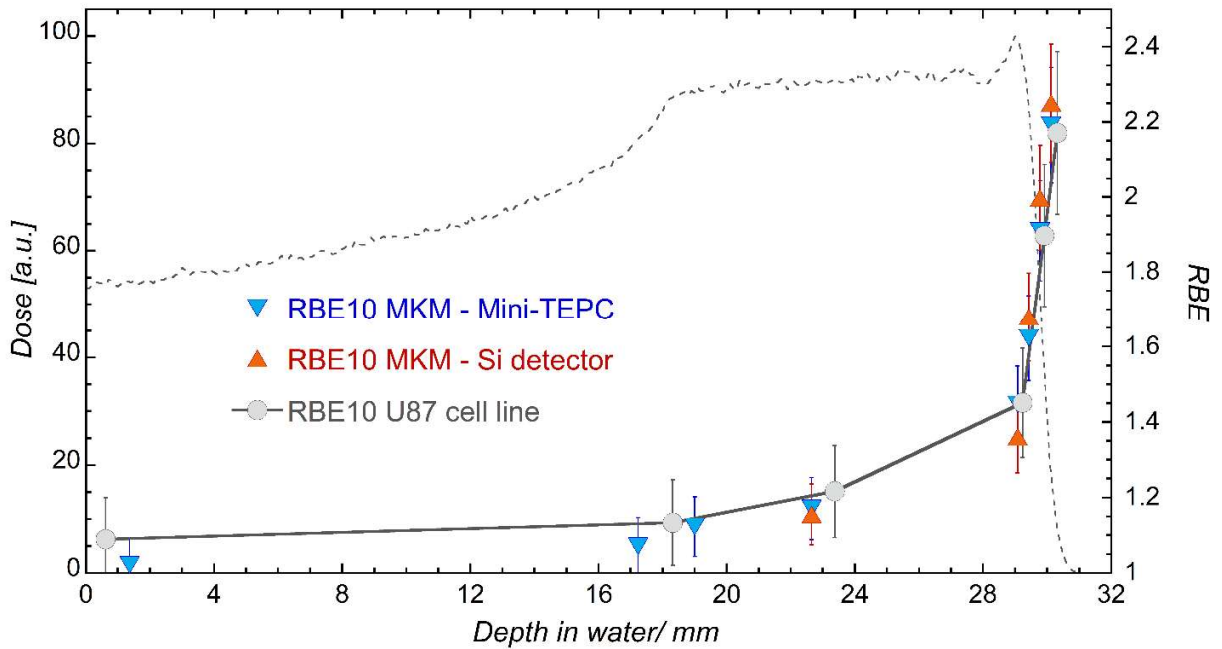


Fig. 9. RBE assessment using the modified MKM.

The mini-TEPC was able to measure even in the entrance part of the SOBP and the RBE10 obtained for these positions with the MKM is also reported in figure 9.

The agreement with biological data is good for both detectors within the uncertainties estimated as 10% for radiobiology data and 7% for the microdosimetric RBE, taking into account the uncertainties on both y^* and α_p .

5. Conclusions

Pairwise measurements were performed at different depths along the 62 MeV SOBP of CATANA, with a sealed mini-TEPC and a silicon telescope of 2 μm thickness. It is confirmed that silicon spectra, when corrected for tissue-equivalence and shape-equivalence, are similar to those produced by a cylindrical mini-TEPC at linear energies higher than 8 keV/ μm . At smaller linear energy values, the signal produced in the 2 μm silicon is too small to be detected due to electronic noise, which was about 16 keV in these measurements. The threshold cut at 8 keV/ μm does not affect seriously the spectra measured in the distal region of the SOBP, because low energy protons have a lineal energy greater than 10 keV/ μm , but it prevents a complete spectral characterization in the entrance and plateau regions because a large fraction of protons have linear energy below the threshold. As a result, microdosimetric spectra extrapolated to 0.1 keV/ μm show significant differences between the two detectors, with the mini-TEPC having a larger fraction of low *LET* events.

The dose mean lineal energy \bar{y}_D for both the mini-TEPC and the silicon microdosimeter shows, as a function of depth in water, a similar trend as the total dose averaged LET. For the mini-TEPC there is also a good numerical agreement, within the 5% uncertainty estimated on \bar{y}_D , whereas for the silicon microdosimeters the measured \bar{y}_D values overestimate the \overline{LET}_d by about a factor of 1.54.

The saturation-corrected dose mean lineal energy, y^* , was used applying the Microdosimetric Kinetic Model to calculate the alpha parameter of the linear quadratic model for human U87 glioblastoma cell survival. Finally, the microdosimetric estimation of RBE10 was derived for both detectors and compared to biological measurements performed on the same radiation field, revealing a good agreement at the investigate depths within the uncertainties, i.e. from the mid position of the SOBP to the fall off.

Acknowledgements

This work was supported by the 5th Scientific Commission of the Italian Institute for Nuclear Physics (INFN), the Belgian nuclear research Centre SCK•CEN and Hasselt University.

This work has been partially supported by the ENEN+ project that has received funding from the EURATOM research and training Work Programme 2016 – 2017 – 1 #755576.

References

- [1] International Commission on Radiation Units and Measurement (ICRU), *Prescribing, Recording, and Reporting Proton Beam Therapy*, Report 78 (2007).
- [2] Paganetti H. *Relative Biological Effectiveness (RBE) values for proton beam therapy. Variations as a function of biological endpoint, dose, and linear energy transfer*. *Phys. Med. Biol.* 59(22), R419–72 (2014).
- [3] Ward J. F., *Biochemistry of DNA Lesions*, *Radiat. Res.* 104 (2s), S103-S111 (1985).
- [4] Wambersie A. et al., *The role of microdosimetry in radiotherapy*, *Radiat. Prot. Dosim.* 31, 421-432 (1990)
- [5] Menzel H. G. et al., *Microdosimetric specification of radiation quality in neutron radiation therapy*, *Int. J. Radiat. Biol.* 57, 865-883 (1990).
- [6] International Commission on Radiation Units and Measurement (ICRU), *Microdosimetry*, Report 36 (1983).
- [7] Rosenfeld A. B. et al., *A new silicon detector for microdosimetry applications in proton therapy*, *IEEE Transactions on Nuclear Science* 47(4), 1386-1394 (2000).
- [8] Agosteo S. et al., *A solid state microdosimeter based on a monolithic silicon telescope*, *Radiat. Prot. Dosim.*, 122(1-4), 382-386 (2006).
- [9] Conte V. et al., *Microdosimetry at the CATANA 62 MeV proton beam with a sealed miniaturized TEPC*, *Phys. Med.* 62, 114-122 (2019).
- [10] Agosteo S. et al., *Study of a silicon telescope for solid state microdosimetry: Preliminary measurements at the therapeutic proton beam line of CATANA*, *Radiat. Meas.* 45, 1284-1289 (2010).
- [11] Kase Y. et al., *Microdosimetric Measurements and Estimation of Human Cell Survival for Heavy-Ion Beams*, *Radiat. Res.* 166, 629-638 (2006).
- [12] Chaudary P. et al., *Relative Biological Effectiveness Along Monoenergetic and Modulated Bragg Peaks of a 62-MeV Therapeutic Proton Beam: A Preclinical Assessment*, *Int. J. Radiat. Oncol. Biol. Phys.* 90 (1), 27-35, (2014).
- [13] De Nardo L. et al., *Mini-TEPCs for Radiation Therapy*, *Radiat. Prot. Dosim.* 108 (4), 345-352 (2004).

- [14] Chiriotti S. et al., *Equivalence of pure propane and propane TE gases for microdosimetric measurements*, Radiat. Prot. Dosim. 166(1-4), 242-246 (2015).
- [15] Ziegler J.F. et al., *SRIM The stopping and range of ions in matter*. Nucl. Instr. Meth. B 268, 1818–1823, (2010).
- [16] Conte V. et al., *Lineal energy calibration of mini tissue equivalent gas- proportional counters (TEPC)*, Multidisciplinary Applications of Nuclear Physics with Ion Beams (ION BEAMS '12) – AIP Conf. Proc. 1530, 171-178 (2013).
- [17] Gerdung S. et al., *Operation and application of Tissue Equivalent Proportional Counters*, Radiat. Prot. Dosim. 61, 381-404 (1995).
- [18] Cirrone G.A.P. et al., *The geant4 toolkit capability in the hadron therapy field: simulation of a transport beam line*. Nucl. Phys. B 150, 54–57 (2005).
- [19] Allison J. et al., *Recent developments in GEANT4*. Nucl. Instrum. Meth. A 835, 186–225 (2016).
- [20] Romano F. et al., *A Monte Carlo study for the calculation of the average linear energy transfer (LET) distributions for a clinical proton beam line and a radiobiological carbon ion beam line*. Phys. Med. Biol. 59, 2863–2882 (2014).
- [21] Petringa G. et al., *Development and analysis of the track-LET, dose-LET and RBE calculations with a therapeutical proton and ion beams using Geant4 Monte Carlo code*. Phys. Med. 42(1), 9 (2017).
- [22] G. A. P Cirrone et al., *A 62-MeV proton beam for the treatment of ocular melanoma at Laboratori Nazionali del Sud-INFN*, IEEE Transactions on Nuclear Science 51(3), 860-865 (2004).
- [23] Kellerer A. M. et al., *The theory of dual radiation action*. Curr. Top. Radiat. Res. 8, 85–158 (1972)
- [24] Debrot E. et al., *SOI microdosimetry and modified MKM for evaluation of relative biological effectiveness for a passive proton therapy radiation field*, Phys. Med. Biol. 63 (2018).
- [25] Magrin G., *Microdosimetry in ion-beam therapy: studying and comparing outcomes from different detectors*, arXiv preprint arXiv:1802.06705 (2018).